

Charged current quasi-elastic scattering of $\bar{\nu}_\mu$ off ^{12}C *

Deepika Grover¹ Kapil Saraswat¹ Prashant Shukla^{2,3} Venktesh Singh^{1;1)}

¹ Department of Physics, Institute of Science, Banaras Hindu University, Varanasi 221005, India

² Nuclear Physics Division, Bhabha Atomic Research Centre, Mumbai 400085, India

³ Homi Bhabha National Institute, Anushakti Nagar, Mumbai 400094, India

Abstract: In this work, we study charged current quasi-elastic scattering (QES) of $\bar{\nu}_\mu$ off nucleon and nucleus using a formalism based on the Llewellyn Smith (LS) model. Parameterizations by Galster et al. are used for electric and magnetic Sachs form factors of the nucleons. We use the Fermi gas model along with the Pauli suppression condition to take into account the nuclear effects in the anti-neutrino–nucleus QES. We calculate $\bar{\nu}_\mu$ - p and $\bar{\nu}_\mu$ - ^{12}C charged current quasi-elastic scattering differential and total cross sections for different values of axial mass M_A , and compare the results with data from the GGM, SKAT, BNL, NOMAD, MINER ν A and MiniBooNE experiments. The present theoretical approach gives a good description of differential cross section data. The calculations with axial mass $M_A=0.979$ and 1.05 GeV are compatible with data from most of the experiments.

Keywords: cross section, quasi-elastic scattering, axial mass, form factors

PACS: 13.15.+g, 25.70.Bc, 96.40.Tv **DOI:** 10.1088/1674-1137/42/12/123104

1 Introduction

From their first postulation by Wolfgang Pauli in 1930, to explain the continuous energy spectra in the beta decay process, neutrinos have been a major field of research. Neutrinos exist in three flavors (electron, muon and tau neutrinos) along with their anti-particles, which are called anti-neutrinos. Searches for more neutrino flavors, called sterile neutrinos, are still underway. The standard model of particle physics assumes (anti)neutrinos to be massless. However, several (anti)neutrino oscillation experiments have confirmed small but non-zero (anti)neutrino masses [1–10]. Being neutral particles, (anti)neutrinos undergo only weak interactions (charged current, via exchange of W^+/W^- bosons, and neutral current, via exchange of Z bosons) with matter, through scattering processes such as quasi-elastic scattering (QES), resonance pion production (RES) and deep inelastic scattering (DIS). For a review see Ref. [11]. In charged current (CC) quasi-elastic scattering (CCQES), an (anti)neutrino interacts with a (proton)neutron, producing a corresponding lepton, and the (proton)neutron changes to a (neutron)proton:

$$\nu_l + n \rightarrow l^- + p, \quad (1)$$

$$\bar{\nu}_l + p \rightarrow l^+ + n. \quad (2)$$

Precise knowledge of (anti)neutrino CCQES is crucial to high energy physics experiments studying neutrino oscillations and hence extracting the neutrino mass hierarchy, mixing angles etc. [1–10]. Several experimental efforts, such as studies at Gargamelle (GGM) [12, 13], SKAT [14], Brookhaven National Laboratory (BNL) [15], Neutrino Oscillation MAgnetic Detector (NOMAD) [16], Main INjector ExpeRiment for ν - A (MINER ν A) [17] and Mini Booster Neutrino Experiment (MiniBooNE) [18] etc. have been performed to describe the quasi-elastic scattering of neutrinos and anti-neutrinos off various nuclear targets. GGM studied quasi-elastic reactions of neutrinos and anti-neutrinos on propane along with a freon target. SKAT bombarded a wide energy band neutrino/anti-neutrino beam onto a heavy freon (CF_3Br) target. BNL used hydrogen (H_2) as a target, NOMAD used carbon, MINER ν A projected an anti-neutrino beam with average energy of 3.5 GeV onto a hydrocarbon target, and MiniBooNE used a mineral oil target. A global analysis of neutrino and anti-neutrino QES differential and total cross sections, along with the extraction of axial mass M_A , is presented in Ref. [19].

In this work, we study charged current anti-neutrino–nucleon and anti-neutrino–nucleus (^{12}C) QES. To describe CCQES, we use the Llewellyn Smith (LS) model [20] and parameterizations by Galster et al. [21]

Received 23 July 2018, Published online 22 October 2018

* Supported by Department of Science and Technology, New Delhi, India

1) E-mail: venkaz@yahoo.com



Content from this work may be used under the terms of the Creative Commons Attribution 3.0 licence. Any further distribution of this work must maintain attribution to the author(s) and the title of the work, journal citation and DOI. Article funded by SCOAP³ and published under licence by Chinese Physical Society and the Institute of High Energy Physics of the Chinese Academy of Sciences and the Institute of Modern Physics of the Chinese Academy of Sciences and IOP Publishing Ltd

for the electric and magnetic Sach's form factors of the nucleons. To incorporate the nuclear effects, in the case of $\bar{\nu}_\mu$ scattering off ^{12}C , we use the Fermi gas model along with the Pauli suppression condition [19, 20, 22–24]. We calculate $\bar{\nu}_\mu-p$ and $\bar{\nu}_\mu-^{12}\text{C}$ CCQES differential and total cross sections for different values of axial mass M_A and compare the results with experimental data, with the goal of finding the most appropriate M_A value. This work does not include the contribution from the 2N2h (two nucleons two holes) effect in QES, where the interaction involves two nucleons producing two holes in the nucleus. Studies of the 2N2h effect in QES are presented in Refs. [25–29].

2 Formalism for quasi-elastic $\bar{\nu}-N$ and $\bar{\nu}-A$ scattering

The Llewellyn Smith model describes (anti)neutrino scattering using a plane wave impulse approximation and calculates the QES cross sections. The anti-neutrino-nucleon charged current quasi-elastic differential cross section for a free nucleon at rest is given as [20]:

$$\frac{d\sigma^{\text{free}}}{dQ^2} = \frac{M_N^2 G_F^2 \cos^2 \theta_c}{8\pi E_\bar{\nu}^2} \times \left[A(Q^2) + \frac{B(Q^2)(s-u)}{M_N^2} + \frac{C(Q^2)(s-u)^2}{M_N^4} \right], \quad (3)$$

where M_N is the nucleon mass, G_F ($=1.16 \times 10^{-5} \text{ GeV}^{-2}$) is the Fermi coupling constant, $\cos \theta_c$ ($=0.97425$) is the Cabibbo angle, and $E_\bar{\nu}$ is the anti-neutrino energy. In terms of the Mandelstam variables s and u , the relation $s-u=4M_N E_\bar{\nu}-Q^2-m_l^2$, where Q^2 is the square of momentum transfer from the anti-neutrino to the outgoing lepton and m_l is the mass of the outgoing lepton.

The functions $A(Q^2)$, $B(Q^2)$ and $C(Q^2)$ are defined as [11, 20, 23]:

$$A(Q^2) = \frac{(m_l^2+Q^2)}{M_N^2} \left\{ \left[(1+\tau)F_A^2 - (1-\tau)(F_1^V)^2 + \tau(1-\tau)(F_2^V)^2 + 4\tau F_1^V F_2^V \right] - \frac{m_l^2}{4M_N^2} \left[(F_1^V + F_2^V)^2 + (F_A + 2F_P)^2 - 4(1+\tau)F_P^2 \right] \right\}, \quad (4)$$

$$B(Q^2) = \frac{Q^2}{M_N^2} F_A (F_1^V + F_2^V), \quad (5)$$

$$C(Q^2) = \frac{1}{4} \left[F_A^2 + (F_1^V)^2 + \tau(F_2^V)^2 \right], \quad (6)$$

where $\tau = \frac{Q^2}{4M_N^2}$. F_A is the axial form factor, F_P is the pseudoscalar form factor and F_1^V , F_2^V are the vector form factors.

The axial form factor F_A is defined in the dipole form as [30]:

$$F_A(Q^2) = \frac{g_A}{\left(1 + \frac{Q^2}{M_A^2}\right)^2}, \quad (7)$$

where g_A ($=-1.267$) is the axial vector constant and M_A is the axial mass.

The pseudoscalar form factor F_P is defined in terms of the axial form factor F_A as [31]:

$$F_P(Q^2) = \frac{2 M_N^2}{Q^2 + m_\pi^2} F_A(Q^2), \quad (8)$$

where m_π is the mass of the pion.

The vector form factors F_1^V and F_2^V are defined as [30, 32]:

$$F_1^V(Q^2) = \frac{1}{(1+\tau)} \left\{ \left[G_E^p(Q^2) - G_E^n(Q^2) \right] + \tau \left[G_M^p(Q^2) - G_M^n(Q^2) \right] \right\}, \quad (9)$$

$$F_2^V(Q^2) = \frac{1}{(1+\tau)} \left\{ \left[G_M^p(Q^2) - G_M^n(Q^2) \right] - \left[G_E^p(Q^2) - G_E^n(Q^2) \right] \right\}, \quad (10)$$

where G_E^p is the electric Sach's form factor of the proton, G_E^n is the electric Sach's form factor of the neutron, G_M^p is the magnetic Sach's form factor of the proton and G_M^n is the magnetic Sach's form factor of the neutron. Several groups such as Galster et al. [21], Budd et al. [33], Bradford et al. [34], Bosted [35] and Alberico et al. [36] provide parameterizations of these form factors by fitting the electron scattering data. For the present calculations, we are using Galster et al.'s parameterizations of these form factors.

The electric and magnetic Sach's form factors of the nucleons are defined as [21]:

$$G_E^p(Q^2) = G_D(Q^2), \quad (11)$$

$$G_M^p(Q^2) = \mu_p G_D(Q^2), \quad (12)$$

$$G_M^n(Q^2) = \mu_n G_D(Q^2). \quad (13)$$

We define the electric Sach's form factor of the neutron using the Krutov and Troitsky [37] parameterization as:

$$G_E^n(Q^2) = -\mu_n \frac{0.942 \tau}{(1+4.61 \tau)} G_D(Q^2), \quad (14)$$

where μ_p ($=2.793$) is the magnetic moment of the proton, μ_n ($=-1.913$) is the magnetic moment of the neutron

and $G_D(Q^2)$ is the dipole form factor, defined as [30]:

$$G_D(Q^2) = \frac{1}{\left(1 + \frac{Q^2}{M_v^2}\right)^2}, \quad (15)$$

where $M_v^2 = 0.71 \text{ GeV}^2$.

The total cross section of anti-neutrino–nucleon (free) quasi-elastic scattering is obtained by integrating the differential cross section, defined by Eq. (3), over Q^2 as [23]:

$$\sigma^{\text{free}}(E_{\bar{\nu}}) = \int_{Q_{\text{min}}^2}^{Q_{\text{max}}^2} dQ^2 \frac{d\sigma^{\text{free}}(E_{\bar{\nu}}, Q^2)}{dQ^2}, \quad (16)$$

where Q_{min}^2 and Q_{max}^2 are defined as:

$$\begin{aligned} Q_{\text{min}}^2 &= -m_l^2 + 2 E_{\bar{\nu}} (E_l - |\vec{k}'|), \\ &= \frac{2E_{\bar{\nu}}^2 M_N - M_N m_l^2 - E_{\bar{\nu}} m_l^2 - E_Q}{2E_{\bar{\nu}} + M_N}, \end{aligned} \quad (17)$$

$$\begin{aligned} Q_{\text{max}}^2 &= -m_l^2 + 2 E_{\bar{\nu}} (E_l + |\vec{k}'|), \\ &= \frac{2E_{\bar{\nu}}^2 M_N - M_N m_l^2 + E_{\bar{\nu}} m_l^2 + E_Q}{2E_{\bar{\nu}} + M_N}. \end{aligned} \quad (18)$$

Here, E_l and \vec{k}' are the energy and momentum of the outgoing lepton, and E_Q is defined as:

$$E_Q = E_{\bar{\nu}} \sqrt{(s - m_l^2)^2 - 2(s + m_l^2)M_N^2 + M_N^4}, \quad (19)$$

where $s = M_N^2 + 2M_N E_{\bar{\nu}}$.

3 Nuclear modifications

For studying anti-neutrino–nucleus quasi-elastic scattering, the nucleus can be treated as a Fermi gas [19, 20, 22–24], where the nucleons move independently within the nuclear volume in an average binding potential generated by all nucleons. The Pauli suppression condition is applied for the nuclear modifications, which implies that the cross section for all the interactions leading to a final state nucleon with a momentum smaller than the Fermi momentum k_F is equal to zero.

The differential cross section per proton for anti-neutrino–nucleus quasi-elastic scattering is defined as [23, 24]:

$$\begin{aligned} &\frac{d\sigma^{\text{nucleus}}(E_{\bar{\nu}}, Q^2)}{dQ^2} \\ &= \frac{2V}{Z(2\pi)^3} \int_0^\infty 2\pi k_p^2 dk_p d(\cos\theta) f(\vec{k}_p) S(\nu - \nu_{\text{min}}) \\ &\quad \times \frac{d\sigma^{\text{free}}(E_{\bar{\nu}}^{\text{eff}}(E_{\bar{\nu}}, k_p), Q^2)}{dQ^2}, \end{aligned} \quad (20)$$

where the factor 2 accounts for the spin of the proton, V is the volume of the nucleus, k_p is the momentum of the proton, $\frac{d\sigma^{\text{free}}}{dQ^2}$ is the differential cross section of the anti-neutrino quasi-elastic scattering off a free proton as

defined by Eq. (3), and $E_{\bar{\nu}}^{\text{eff}}$ is the effective anti-neutrino energy in the presence of Fermi motion of nucleons.

$E_{\bar{\nu}}^{\text{eff}}$ is defined as [23]:

$$E_{\bar{\nu}}^{\text{eff}} = \frac{(s^{\text{eff}} - M_p^2)}{2M_p}. \quad (21)$$

Here, M_p is the proton mass and s^{eff} is defined as [23]:

$$s^{\text{eff}} = M_p^2 + 2E_{\bar{\nu}} \left(E_p - k_p \cos\theta \right), \quad (22)$$

where E_p is the proton energy, defined as:

$$E_p = \sqrt{k_p^2 + M_p^2}. \quad (23)$$

The Fermi distribution function $f(\vec{k}_p)$ is defined as:

$$f(\vec{k}_p) = \frac{1}{1 + \exp\left(\frac{k_p - k_F}{a}\right)}, \quad (24)$$

where $a = kT$ ($= 0.020 \text{ GeV}$) is the diffuseness parameter [24]. The Fermi momentum k_F for the carbon nucleus is 0.221 GeV [38].

The Pauli suppression factor $S(\nu - \nu_{\text{min}})$ is defined as [23, 24]:

$$S(\nu - \nu_{\text{min}}) = \frac{1}{1 + \exp\left(-\frac{(\nu - \nu_{\text{min}})}{a}\right)}, \quad (25)$$

where ν is the energy transfer in the interaction, defined as:

$$\nu = (Q^2 + M_n^2 - M_p^2) / (2M_p), \quad (26)$$

and ν_{min} is defined as:

$$\nu_{\text{min}} = \sqrt{k_F^2 + M_n^2} - \sqrt{k_p^2 + M_p^2} + E_B. \quad (27)$$

Here, M_n is the final state neutron mass and E_B is the binding energy. For the carbon nucleus, $E_B = 10 \text{ MeV}$ [24].

The total cross section of anti-neutrino–nucleus quasi-elastic scattering is obtained by integrating the differential cross section, as defined by Eq. (20), over Q^2 , where Q^2 ranges from Q_{min}^2 to Q_{max}^2 defined by Eqs. (17) and (18), calculated with $E_{\bar{\nu}}^{\text{eff}}$ instead of $E_{\bar{\nu}}$.

4 Results and discussion

We calculated the charged current $\bar{\nu} - N$ and $\bar{\nu} - A$ quasi-elastic differential scattering cross sections. Figure 1 shows the present calculations of $\bar{\nu}_\mu - p$ charged current quasi-elastic differential scattering cross section $\frac{d\sigma}{dQ^2}$ as a function of the square of momentum transfer Q^2 , for different values of axial mass ($M_A = 0.979, 1.05, 1.12$ and 1.23 GeV) and for anti-neutrino energy $E_{\bar{\nu}} = 2 \text{ GeV}$. The value of differential cross section increases with increasing axial mass.

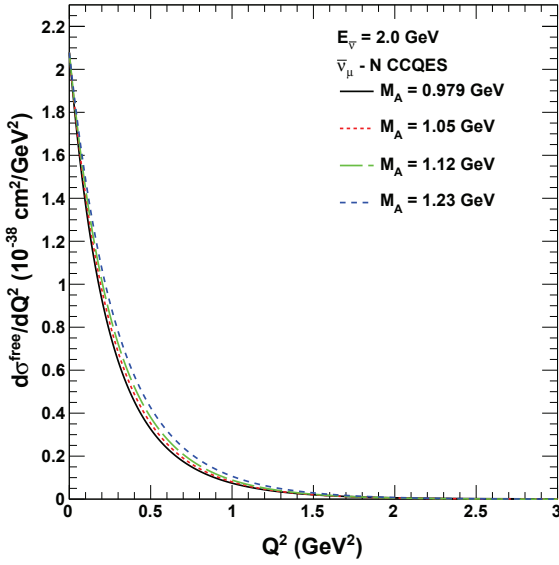


Fig. 1. (color online) Differential cross section $\frac{d\sigma}{dQ^2}$ for $\bar{\nu}_\mu-p$ charged current QES as a function of the square of momentum transfer Q^2 , for different values of axial mass M_A and for anti-neutrino energy $E_{\bar{\nu}}=2$ GeV.

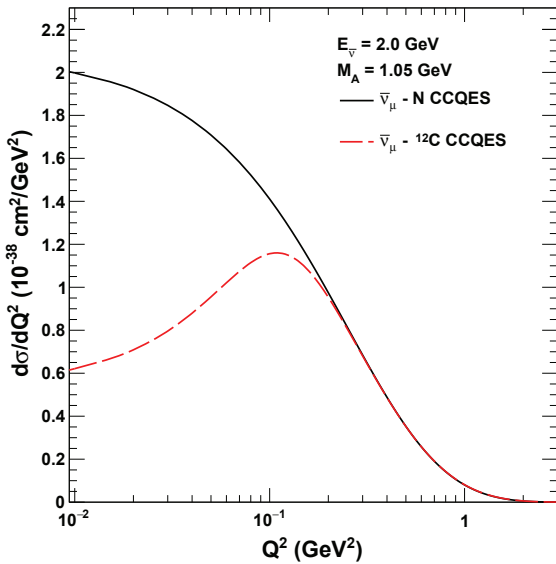


Fig. 2. (color online) Differential cross section $\frac{d\sigma}{dQ^2}$ for $\bar{\nu}_\mu-p$ and $\bar{\nu}_\mu-^{12}\text{C}$ charged current QES as a function of the square of momentum transfer Q^2 , for axial mass $M_A=1.05$ GeV and for anti-neutrino energy $E_{\bar{\nu}}=2$ GeV.

Figure 2 shows the differential cross section $\frac{d\sigma}{dQ^2}$ for $\bar{\nu}_\mu-p$ and $\bar{\nu}_\mu-^{12}\text{C}$ charged current QES as a function of the square of momentum transfer Q^2 , with axial mass

$M_A=1.05$ GeV and anti-neutrino energy $E_{\bar{\nu}}=2$ GeV. The anti-neutrino-carbon cross section is lower than the anti-neutrino-proton cross section for smaller values of Q^2 due to nuclear effects. The cross sections gradually drop to zero with increasing value of Q^2 .

We compared the present calculations of $\bar{\nu}_\mu-^{12}\text{C}$ charged current quasi-elastic differential scattering cross section with experimental data from several collaborations. Figure 3 shows the flux-integrated differential cross section $\frac{d\sigma}{dQ^2}$ per proton for anti-neutrino-carbon CCQES as a function of the square of momentum transfer Q^2 corresponding to the MiniBooNE data [18], measuring the muon anti-neutrino CCQES cross section off a mineral oil (carbon) target. The calculations are performed for different values of axial mass ($M_A=0.979, 1.05, 1.12$ and 1.23 GeV). The average anti-neutrino energy $\langle E_{\bar{\nu}} \rangle = 665$ MeV. The calculations with axial mass $M_A=0.979$ and 1.05 GeV are compatible with data.

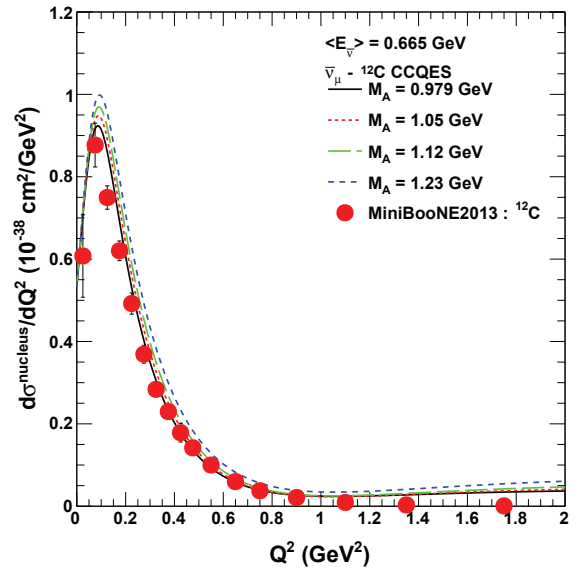


Fig. 3. (color online) Flux-integrated differential cross section $\frac{d\sigma}{dQ^2}$ per proton for $\bar{\nu}_\mu-^{12}\text{C}$ charged current QES as a function of the square of momentum transfer Q^2 corresponding to the MiniBooNE data [18]. The average anti-neutrino energy $\langle E_{\bar{\nu}} \rangle = 665$ MeV.

Figure 4 shows the differential cross section $\frac{d\sigma}{dQ^2}$ per proton for anti-neutrino-carbon CCQES as a function of the square of momentum transfer Q^2 , for different values of axial mass ($M_A=0.979, 1.05, 1.12$ and 1.23 GeV) and for average anti-neutrino energy $\langle E_{\bar{\nu}} \rangle = 2$ GeV. The results obtained are compared with data from Gargamelle (GGM) [12], which studied quasi-elastic reactions of neutrinos and antineutrinos on a propane plus freon target.

The calculations with axial mass $M_A = 0.979$ and 1.05 GeV are compatible with data.

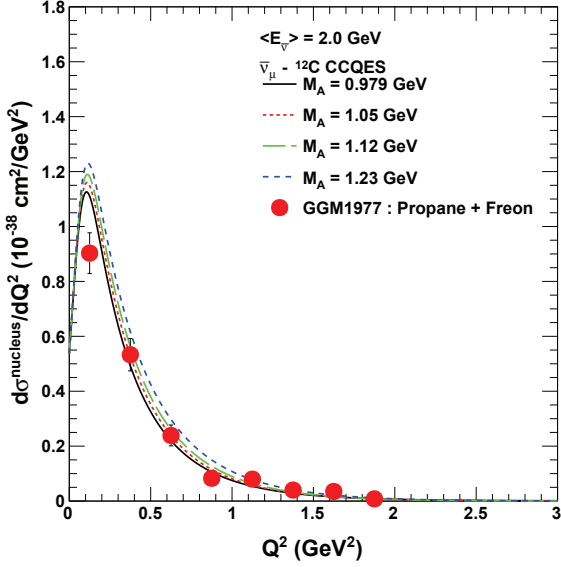


Fig. 4. (color online) Differential cross section $\frac{d\sigma}{dQ^2}$ per proton for $\bar{\nu}_\mu$ - ^{12}C charged current QES as a function of the square of momentum transfer Q^2 , for different values of axial mass M_A and for average anti-neutrino energy $\langle E_{\bar{\nu}} \rangle = 2$ GeV compared with GGM data [12].

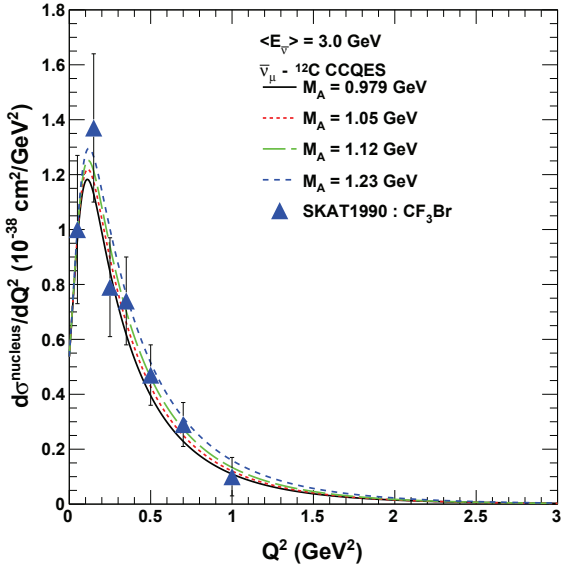


Fig. 5. (color online) Differential cross section $\frac{d\sigma}{dQ^2}$ per proton for $\bar{\nu}_\mu$ - ^{12}C charged current QES as a function of the square of momentum transfer Q^2 , for different values of axial mass M_A and for average anti-neutrino energy $\langle E_{\bar{\nu}} \rangle = 3$ GeV compared with SKAT data [14].

Figure 5 shows the differential cross section $\frac{d\sigma}{dQ^2}$ per proton for anti-neutrino-carbon CCQES as a function of the square of momentum transfer Q^2 , for different values of axial mass ($M_A = 0.979, 1.05, 1.12$ and 1.23 GeV) and for average anti-neutrino energy $\langle E_{\bar{\nu}} \rangle = 3$ GeV. The results obtained are compared with SKAT data [14] studying the cross sections of neutrino and anti-neutrino quasi elastic interactions using a wide energy band (3 - 30 GeV) neutrino/anti-neutrino beam on a heavy freon (CF_3Br) target. The calculations with axial mass $M_A = 0.979$ and 1.05 GeV are compatible with data.

Figure 6 shows the differential cross section $\frac{d\sigma}{dQ^2}$ per proton for anti-neutrino-carbon CCQES as a function of the square of momentum transfer Q^2 , for different values of axial mass ($M_A = 0.979, 1.05, 1.12$ and 1.23 GeV). The results obtained are compared with MINER ν A data [17] measuring muon anti-neutrino quasi-elastic scattering on a hydrocarbon target at $\langle E_{\bar{\nu}} \rangle = 3.5$ GeV. The calculation with axial mass $M_A = 0.979$ GeV is compatible with data.

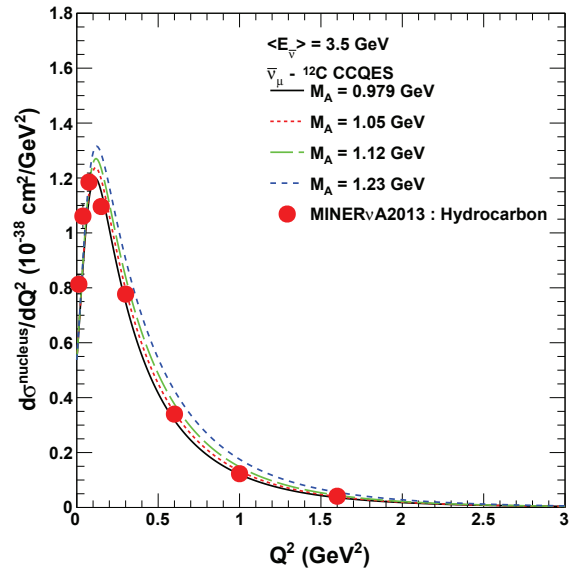


Fig. 6. (color online) Differential cross section $\frac{d\sigma}{dQ^2}$ per proton for $\bar{\nu}_\mu$ - ^{12}C charged current QES as a function of the square of momentum transfer Q^2 , for different values of axial mass M_A and for average anti-neutrino energy $\langle E_{\bar{\nu}} \rangle = 3.5$ GeV compared with MINER ν A data [17].

We calculated the total cross section for charged current $\bar{\nu}$ - N and $\bar{\nu}$ - A quasi elastic scattering and compared the present results with data from several experiments. Figure 7 shows the present calculations of the total cross section σ for anti-neutrino-proton CCQES as a function of the anti-neutrino energy $E_{\bar{\nu}}$, for different values of axial mass ($M_A = 0.979, 1.05, 1.12$ and 1.23 GeV). The

value of total cross section increases with increasing axial mass. We compared the obtained results with data from the BNL [15] and NOMAD [16] experiments. The calculation with axial mass $M_A=1.05$ GeV is compatible with data.

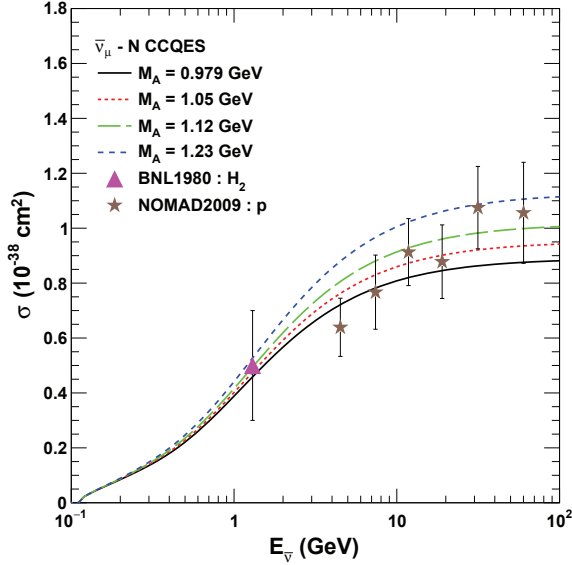


Fig. 7. (color online) Total cross section σ for $\bar{\nu}_\mu-p$ CCQES as a function of the anti-neutrino energy $E_{\bar{\nu}}$, for different values of axial mass M_A compared with BNL [15] and NOMAD [16] data.

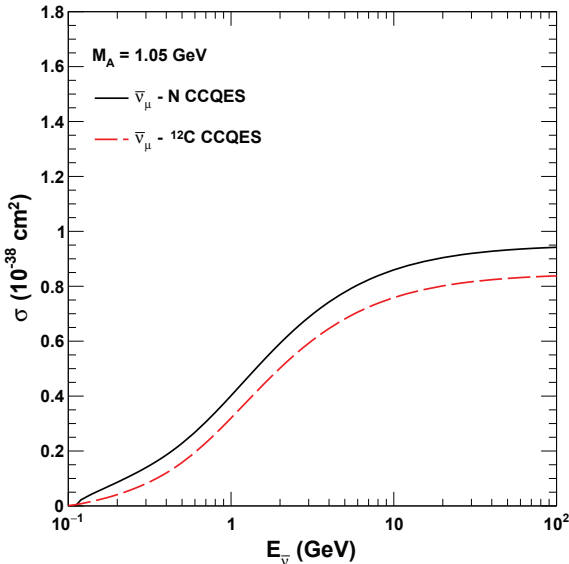


Fig. 8. (color online) Total cross section σ for $\bar{\nu}_\mu-p$ and $\bar{\nu}_\mu-^{12}\text{C}$ charged current quasi-elastic scattering as a function of the anti-neutrino energy $E_{\bar{\nu}}$, for axial mass $M_A=1.05$ GeV.

Figure 8 shows the total cross section σ for $\bar{\nu}_\mu-p$ and $\bar{\nu}_\mu-^{12}\text{C}$ charged current QES as a function of the anti-neutrino energy $E_{\bar{\nu}}$, with axial mass $M_A=1.05$ GeV. The nuclear effects reduce the anti-neutrino-carbon cross section compared to the anti-neutrino-proton cross section.

Figure 9 shows the total cross section σ per proton for $\bar{\nu}_\mu-^{12}\text{C}$ charged current QES as a function of the anti-neutrino energy $E_{\bar{\nu}}$, for different values of axial mass ($M_A=0.979, 1.05, 1.12$ and 1.23 GeV). The results obtained are compared with data from the GGM(1977) [12], GGM(1979) [13], SKAT [14], NOMAD [16] and MiniBooNE [18] experiments. The calculations with axial mass $M_A=0.979$ and 1.05 GeV are compatible with the GGM(1977), GGM(1979) and SKAT data, though the calculations overestimate the data at low anti-neutrino energies. The approach parameterizing axial mass M_A as a function of anti-neutrino energy, presented in Ref. [39], can be used to get a better agreement with data at low anti-neutrino energies. The calculation with axial mass $M_A=1.05$ GeV is compatible with NOMAD data and the calculation with axial mass $M_A=1.23$ GeV is compatible with MiniBooNE data.

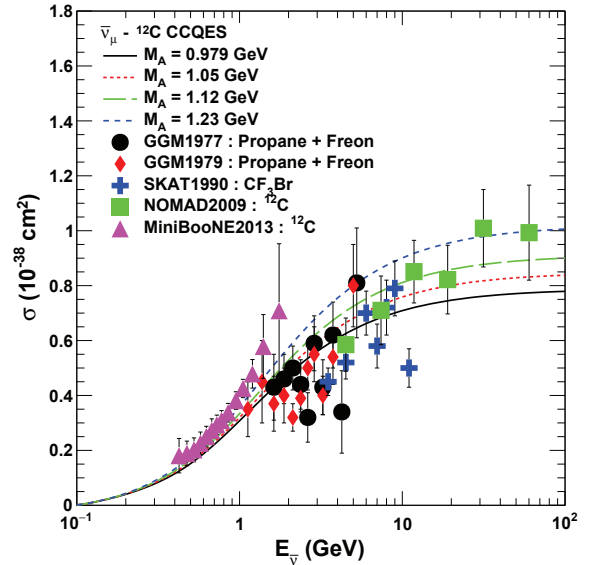


Fig. 9. (color online) Total cross section σ per proton for $\bar{\nu}_\mu-^{12}\text{C}$ charged current QES as a function of the anti-neutrino energy $E_{\bar{\nu}}$, for different values of axial mass M_A compared with GGM(1977) [12], GGM(1979) [13], SKAT [14], NOMAD [16] and MiniBooNE [18] data.

5 Conclusion

We have presented a study on charged current anti-neutrino-nucleon and anti-neutrino-nucleus (carbon) quasi-elastic scattering using the Llewellyn Smith

(LS) model. For the electric and magnetic Sach's form factors of nucleons, we used Galster et al.'s parameterizations. The Fermi gas model, along with the Pauli suppression condition, has been used to incorporate the nuclear effects in anti-neutrino–nucleus QES. We calculated $\bar{\nu}_\mu-p$ and $\bar{\nu}_\mu-^{12}\text{C}$ charged current quasi-elastic differential and total scattering cross sections for different

values of axial mass M_A and compared the obtained results with data from the GGM, SKAT, BNL, NOMAD, MINER ν A and MiniBooNE experiments. The present theoretical approach gives a good description of differential cross section data. The calculations with axial mass $M_A=0.979$ and 1.05 GeV are compatible with data from most of the experiments.

References

- 1 M. H. Ahn et al (K2K Collaboration), Phys. Rev. Lett., **90**: 041801 (2003)
- 2 E. Aliu et al (K2K Collaboration), Phys. Rev. Lett., **94**: 081802 (2005)
- 3 M. H. Ahn et al (K2K Collaboration), Phys. Rev. D, **74**: 072003 (2006)
- 4 Y. Ashie et al (Super-Kamiokande Collaboration), Phys. Rev. D, **71**: 112005 (2005)
- 5 Y. Takeuchi (Super-Kamiokande Collaboration), Nucl. Phys. Proc. Suppl., **79**: 229 - 232 (2012)
- 6 P. Adamson et al (NOvA Collaboration), Phys. Rev. Lett., **116**(15): 151806 (2016)
- 7 P. Adamson et al (NOvA Collaboration), Phys. Rev. D, **93**(5): 051104 (2016)
- 8 P. Adamson et al (NOvA Collaboration), Phys. Rev. Lett., **118**(15): 151802 (2017)
- 9 P. Adamson et al (NOvA Collaboration), Phys. Rev. Lett., **118**(23): 231801 (2017)
- 10 S. Ahmed et al (ICAL Collaboration), Pramana, **88**(5): 79 (2017)
- 11 J. A. Formaggio and G. P. Zeller, Rev. Mod. Phys., **84**: 1307 (2012)
- 12 S. Bonetti, G. Carnesecchi, D. Cavalli, P. Negri, A. Pullia, M. Rollier, F. Romano, and R. Schira, Nuovo Cim. A, **38**: 260 (1977)
- 13 N. Armenise et al, Nucl. Phys. B, **152**: 365 (1979)
- 14 J. Brunner et al (SKAT Collaboration), Z. Phys. C, **45**: 551 (1990)
- 15 G. Fanourakis et al, Phys. Rev. D, **21**: 562 (1980)
- 16 V. Lyubushkin et al (NOMAD Collaboration), Eur. Phys. J. C, **63**: 355 (2009)
- 17 L. Fields et al (MINER ν A Collaboration), Phys. Rev. Lett., **111**(2): 022501 (2013)
- 18 A. A. Aguilar-Arevalo et al (MiniBooNE Collaboration), Phys. Rev. D, **88**(3): 032001 (2013)
- 19 K. S. Kuzmin, V. V. Lyubushkin, and V. A. Naumov, Eur. Phys. J. C, **54**: 517 (2008)
- 20 C. H. Llewellyn Smith, Phys. Rept., **3**: 261 (1972)
- 21 S. Galster, H. Klein, J. Moritz, K. H. Schmidt, D. Wegener, and J. Bleckwenn, Nucl. Phys. B, **32**: 221 (1971)
- 22 R. A. Smith and E. J. Moniz, Nucl. Phys. B, **43**: 605 (1972) Erratum: [Nucl. Phys. B, **101**: 547 (1975)]
- 23 Amin A. Leghrouz, M. A. Abu-Samreh, and A. M. Saleh, J. Al-Aqsa Univ., **10**(S.E.), (2006)
- 24 K. Saraswat, P. Shukla, V. Kumar, and V. Singh, Indian J. Phys., **92**(2): 249 (2018)
- 25 L. Alvarez-Ruso, Y. Hayato, and J. Nieves, New J. Phys., **16**: 075015 (2014)
- 26 R. Gran, J. Nieves, F. Sanchez, and M. J. Vicente Vacas, Phys. Rev. D, **88**(11): 113007 (2013)
- 27 M. Martini, M. Ericson, G. Chanfray, and J. Marteau, Phys. Rev. C, **80**: 065501 (2009)
- 28 M. Martini, M. Ericson, G. Chanfray, and J. Marteau, Phys. Rev. C, **81**: 045502 (2010)
- 29 M. Martini, M. Ericson, and G. Chanfray, Phys. Rev. C, **84**: 055502 (2011)
- 30 P. Stoler, Phys. Rept., **226**: 103 (1993)
- 31 V. Bernard, L. Elouadrhiri, and U. G. Meissner, J. Phys. G, **28**: R1 (2002)
- 32 H. S. Budd, A. Bodek, and J. Arrington, hep-ex/0308005
- 33 H. S. Budd, A. Bodek, and J. Arrington, Nucl. Phys. Proc. Suppl., **139**: 90 (2005)
- 34 R. Bradford, A. Bodek, H. S. Budd, and J. Arrington, Nucl. Phys. Proc. Suppl., **159**: 127 (2006)
- 35 P. E. Bosted, Phys. Rev. C, **51**: 409 (1995)
- 36 W. M. Alberico, S. M. Bilenky, C. Giunti, and K. M. Graczyk, Phys. Rev. C, **79**: 065204 (2009)
- 37 A. F. Krutov and V. E. Troitsky, Eur. Phys. J. A, **16**: 285 (2003)
- 38 E. J. Moniz, I. Sick, R. R. Whitney, J. R. Ficenc, R. D. Kephart, and W. P. Trower, Phys. Rev. Lett., **26**: 445 (1971)
- 39 L. D. Kolupaeva, K. S. Kuzmin, O. N. Petrova, and I. M. Shandrov, Mod. Phys. Lett. A, **31**(12): 1650077 (2016)